

Age of Entanglement in Satellite Repeater Chains with Intermittent Availability

Elif Tugce Ceran

Department of Electrical and Electronics Engineering
Faculty of Engineering, Middle East Technical University
Ankara, Turkey
elifce@metu.edu.tr

Abstract—Timely availability of high-fidelity entanglement is essential for emerging quantum networks. This paper introduces the Age of Entanglement (AoE) as a novel performance metric that captures the freshness of bipartite entanglement under continuous distribution in quantum repeater chains. AoE extends classical Age of Information (AoI) based metrics to quantum networking by capturing storage, decoherence, probabilistic entanglement generation and swapping.

We study a satellite-assisted quantum repeater network in which entangled pairs are generated probabilistically, stored in quantum memories suffer from decoherence, and combined to form end-to-end entangled links. Satellite-ground connectivity is intermittent and modeled as a two-state Markov chain. The resulting AoE minimization problem is formulated as an infinite-horizon Markov decision process (MDP), where control actions determine when to generate, store, or swap entangled pairs under stochastic link availability and memory degradation.

Using relative value iteration, we characterize AoE-optimal policies and evaluate their performance numerically. Our results highlight the impact of decoherence, imperfect operations, and visibility dynamics, and show that the proposed dynamic policies significantly outperform swap-as-soon-as-possible and greedy entanglement generation strategies. Our results provide practical design and control guidelines for satellite-enabled quantum repeater chains supporting continuous entanglement distribution.

I. INTRODUCTION

The development of quantum communication networks is reshaping communication and computation by enabling secure quantum-enabled applications [1]. These networks support tasks such as quantum teleportation and quantum key distribution (QKD) [1], [2], [3]. Bipartite entanglement constitutes the essential resource for these tasks, providing a quantum link between spatially separated nodes. However, photon loss in optical fibers limits the direct distribution of entanglement over long distances. To address this challenge, quantum repeaters and satellite-based nodes are employed to extend entanglement distribution to global scales.

Classical communication achieves reliability through coding and retransmission of bits over noisy channels, whereas quantum communication is fundamentally constrained by principles such as the no-cloning theorem. As a result, quantum communication often relies on shared entanglement between distant nodes. In repeater-based networks, entanglement is typically generated probabilistically between neighboring nodes and confirmed via classical signaling, then extended over

longer distances through entanglement swapping at intermediate nodes. Since stored quantum states are highly sensitive to noise and decohere over time, their quality degrades as they age.

Satellite-based quantum networks offer a distinct advantage for long-distance entanglement distribution by exploiting low-loss free-space optical channels [2], [3], [4]. However, they are constrained by intermittent visibility and limited contact durations due to orbital dynamics and onboard resource constraints. Despite these advantages, entanglement distribution remains challenged by the time sensitivity of quantum states and the inherently probabilistic nature of generating entanglement between neighboring nodes and combining shorter entangled links to form end-to-end links with swapping.

To quantify the freshness of quantum resources, we introduce the Age of Entanglement (AoE) as a performance metric, inspired by the classical Age of Information (AoI) [5], [6]. In classical networks, AoI resets to the age of the most recently delivered update. Similarly, AoE resets upon successful generation of an end-to-end entangled link; however, it must additionally capture quantum-specific effects such as decoherence and imperfect entanglement generation and swapping, which accumulate while qubits are stored and processed. AoE provides a natural framework for designing control policies that jointly account for probabilistic operations, memory aging, and intermittent connectivity in satellite-based quantum networks.

A. Related Work

Entanglement distribution protocols are typically classified as on-demand or continuous distribution (CD) schemes [7], [8]. On-demand approaches [9], [10], [11] establish links only upon request and can incur scheduling overhead as networks scale. In contrast, CD protocols proactively supply entanglement, enabling background applications such as QKD and faster resource allocation in heterogeneous networks. Recent adaptive CD schemes further reduce service latency by leveraging information from prior requests [7], [8].

Satellite-based quantum networks, such as entanglement distribution using hybrid links (ED-HL), combine satellite downlinks, inter-satellite links, and onboard quantum memories to enable global-scale entanglement distribution, with resource allocation typically formulated as an integer program-

ming problem under link availability and resource constraints [4].

Quantum network dynamics are well-suited for modeling as Markov decision processes (MDPs) [12] and previous work leveraged MDPs [9], [10], [13] and dynamic programming to optimize entanglement distribution policies. Recent research has also employed reinforcement learning (RL), such as Q-learning, to discover hardware-aware policies that outperform the standard swap-as-soon-as-possible (SWAP-ASAP) approach [9] and address non-linear application-driven objectives [10].

On the other hand, Age of Information (AoI) based policies have demonstrated significant gains in semantic and goal-oriented classical communication, as AoI is a well-established metric for capturing the freshness of data updates while jointly accounting for delay and throughput [5], [6]. Minimizing AoI has been widely modeled as a MDP, and state-dependent dynamic policies have been shown to be highly effective in prior work [14], [15].

To the best of our knowledge, while link ages have been employed as state variables and fidelity indicators in prior works, the Age of Entanglement (AoE) of the end-to-end link has not been explicitly formulated. Moreover, the relationship and fundamental differences between the classical AoI for data packets and the AoE for entangled quantum links have not been systematically characterized.

The main contributions of this paper are as follows:

- We introduce a novel modeling framework that, for the first time, captures intermittent availability of repeater nodes in quantum entanglement distribution.
- We propose a state-dependent dynamic control policy for entanglement generation and swapping that significantly outperforms stationary heuristics such as swap-as-soon-as-possible and greedy regeneration.
- We formalize the Age of Entanglement (AoE) metric, inspired by the AoI, to jointly capture entanglement generation delay and quality degradation due to decoherence.

II. SYSTEM MODEL

We consider a discrete-time and slotted linear quantum repeater network for distributing bipartite entanglement between two ground stations, *Alice* and *Bob*, via satellite-based repeater nodes. A shared bipartite entangled state between two nodes is referred to as an entangled link. Satellites act as intermediate repeaters that relay entanglement between neighboring nodes to enable long-distance quantum communication. In this work, we focus on the single-repeater case, where one satellite (node 2) serves as the intermediate node between *Alice* (node 1) and *Bob* (node 3).

Satellite-to-ground connectivity is inherently intermittent due to orbital motion and elevation-angle constraints. A communication link between a ground station and a satellite is available only when the satellite exceeds a minimum elevation angle θ_e , ensuring sufficient link quality. An elementary link is a heralded bipartite entangled state established via direct physical downlinks between a satellite source and each of its

visible ground stations. A virtual end-to-end link is a logical connection generated between physically non-neighboring ground nodes through entanglement swapping operations performed by intermediate satellite repeater.

We model the visibility of each ground–satellite link as a two-state Markov process with state space $V \in \{0, 1\}$, where 0 and 1 denote the invisible and visible states, respectively. An elementary entangled link between node i and satellite j can be established at time slot t only if $v_t^{ij} = 1$. Let $v_t^{12} \in \{0, 1\}$ and $v_t^{23} \in \{0, 1\}$ denote the visibility states of links (1, 2) and (2, 3), respectively. When $v_t^{ij} = 1$, the corresponding elementary link is available and nodes can request elementary link generation at time t ; otherwise, it is unavailable.

To provide high fidelity and timely end-to-end entanglement link between the two end nodes, we assume the nodes can perform the following operations at each time slot: i) heralded generation of entanglement between each ground node and intermittently available satellite, which succeeds with probability p_L , and discarding any link that existed before attempt, ii) entanglement swap attempts, which consumes two adjacent entangled links to generate a longer distance link between ground nodes with probability p_s and iii) waiting for a better opportunity to generate or swap in the future and letting the links decohere. We also adopt a common assumption and assume discarding any link that existed for some time denoted by m^* and emptying qubit resources to prevent generation of low-quality end-to-end entanglement due to decoherence.

In real quantum memories, the stored entangled state degrades over time due to decoherence, and its fidelity $F(m)$, defined as the closeness between the noisy state and the ideal state, typically decays with storage time m ; for example, in simple phase-damping models the fidelity of a stored entangled pair decreases approximately exponentially as

$$F(m) \approx e^{-m/T_2}, \quad (1)$$

where T_2 is the memory coherence time that characterizes how rapidly phase information is lost. Consequently, larger link ages correspond to less fidelity, which motivates the use of age-based policies to avoid poor-quality end-to-end entanglement as commonly adopted in previous work [9].

Let m_t^{12} and m_t^{23} denote the ages of the elementary links (1, 2) and (2, 3) at time t , respectively. Each elementary-link age takes values in the set $\{-1, 1, 2, \dots, m^*\}$, where -1 represents an inactive (non-existent) link and positive integers represent the number of time slots elapsed since the entanglement was generated. Newly generated elementary links are initialized with age equal to 1; consequently, age 0 never occurs. If an elementary link age exceeds the cutoff m^* , the corresponding entanglement is discarded and the age is reset to -1 .

A. Age of Entanglement (AoE)

We introduce the *Age of Entanglement (AoE)* as a performance metric that captures the freshness of the most recently generated end-to-end entangled pair between nodes 1 and 3.

Note that, unlike the Age of Information (AoI) used for elementary links, the AoE is not associated with the presence or absence of a physical quantum state, but instead records the time elapsed since the last successful creation of an end-to-end entangled link. The AoE captures both the elapsed time since the most recent successful end-to-end entanglement generation and the degradation of the resulting entangled state due to aging and decoherence, whereas the AoI is a classical metric used to quantify the freshness of information packets.

Let Δ_t^e denote the AoE at the beginning of the time slot t . The AoE evolves stochastically with time depending on the control actions and successful swap probabilities and is updated as follows:

- If an entanglement swapping operation is successfully performed at time t with probability p_s , producing an end-to-end entangled pair using elementary links with ages m_t^{12} and m_t^{23} , then the AoE is *reset* according to

$$\Delta_{t+1}^e = m_t^{12} + m_t^{23}. \quad (2)$$

This update reflects the standard entanglement swapping formalism in quantum repeaters [9], where the swapped state inherits the accumulated storage induced decoherence of the elementary links.

- If no successful end-to-end entanglement is generated at time t , then the AoE increases by one unit:

$$\Delta_{t+1}^e = \Delta_t^e + 1. \quad (3)$$

The AoE thus represents the age of the most recent end-to-end entanglement, regardless of whether an entangled pair is currently available. Between successive successful swapping events, the AoE grows linearly with time, and it is reset to a value that reflects the freshness of the elementary links used to generate the end-to-end entanglement.

This formulation differs fundamentally from terminal or episodic models, as the system continues to operate after each successful end-to-end entanglement generation. Consequently, AoE provides a natural objective for continuing-control formulations, allowing policies to trade off the frequency of successful entanglement generation (or end-to-end entanglement generation delay) against the freshness of the resulting end-to-end links.

Problem. *The objective is to determine a stationary policy π that minimizes the infinite horizon expected average AoE*

$$\eta^\pi \triangleq \liminf_{T \rightarrow \infty} \frac{1}{T} \mathbb{E}_\pi \left[\sum_{t=0}^{T-1} \Delta_{t+1}^e \right]. \quad (4)$$

III. MDP FORMULATION AND RVI

A. Markov Decision Process Formulation

We model the operation of a three-node linear quantum repeater chain as a discrete-time average reward Markov decision process (MDP) with tuple $\langle \mathcal{S}, \mathcal{A}, P, r \rangle$ [12]. The network consists of nodes 1–2–3, where entanglement can be generated on the elementary links (1, 2) and (2, 3), and an end-to-end virtual link (1, 3) can be established via entanglement swapping at the intermediate node 2.

1) *State Space:* At time slot t , the system state is

$$s_t \triangleq (v_t^{12}, v_t^{23}, m_t^{12}, m_t^{23}, \Delta_t^e) \in \mathcal{S}, \quad (5)$$

where $v_t^{12} \in \{0, 1\}$ and $v_t^{23} \in \{0, 1\}$ denote the visibility states associated with links (1, 2) and (2, 3), respectively. A value of $v_t^{ij} = 1$ indicates that the corresponding elementary link can be requested at time t , while $v_t^{ij} = 0$ indicates that the link is not visible.

The variable Δ_t^e denotes the AoE of the end-to-end link (1, 3), representing the age of the most recently generated end-to-end entangled pair. The AoE takes values in $\{1, 2, \dots, \Delta_{\max}^e\}$, and Δ_t^e increases by one every time slot until the next successful end-to-end entanglement generation. To ensure a finite state space, the AoE is capped at a large constant Δ_{\max}^e , i.e., once Δ_t^e reaches Δ_{\max}^e it remains at Δ_{\max}^e until the next successful reset.

In contrast to episodic or on-demand entanglement generation policies, the MDP is continuing, that is, there are no terminal or absorbing states, and the process evolves indefinitely.

2) *Action Space:* At each time slot t , the controller selects an action

$$a_t \triangleq (a_t^{12}, a_t^{23}, a_t^{\text{sw}}) \in \mathcal{A}, \quad (6)$$

where $a_t^{12} \in \{0, 1\}$ and $a_t^{23} \in \{0, 1\}$ indicate whether a request is made to generate entanglement on links (1, 2) and (2, 3), respectively, and $a_t^{\text{sw}} \in \{0, 1\}$ indicates whether an entanglement swapping operation is attempted at node 2.

Not all actions are admissible in every state, i.e., $a_t \in \mathcal{A}(s)$, where $\mathcal{A}(s)$ represents the admissible policies for each state $s_t = s$. Specifically, entanglement swapping cannot be performed simultaneously with link generation, that is, if $a_t^{\text{sw}} = 1$, then $a_t^{12} = a_t^{23} = 0$.

Moreover, link generation requests are gated by visibility, such that $a_t^{12} = 1$ requires $v_t^{12} = 1$, and $a_t^{23} = 1$ requires $v_t^{23} = 1$. Finally, a swap action is feasible only if both elementary links exist, i.e., $a_t^{\text{sw}} = 1$ requires $m_t^{12} \geq 1$ and $m_t^{23} \geq 1$.

3) *Visibility Dynamics:* The satellite visibility processes evolve exogenously and independently of the control actions. Specifically, v_t^{12} and v_t^{23} each follow a two-state Markov chain with transition probabilities

$$\begin{aligned} \Pr(v_{t+1}^{12} = j \mid v_t^{12} = i) &= [\mathbf{P}_{12}]_{i,j}, \\ \Pr(v_{t+1}^{23} = j \mid v_t^{23} = i) &= [\mathbf{P}_{23}]_{i,j}, \end{aligned} \quad (7)$$

for $i, j \in \{0, 1\}$, where \mathbf{P}_{12} and \mathbf{P}_{23} are given 2×2 stochastic matrices.

4) *State Transitions:* The one-step transition probability $P(s_{t+1} \mid s_t, a_t)$ factorizes into visibility transition probabilities as in (7) and link-state transitions as follows.

When a swap is attempted, $a_t^{\text{sw}} = 1$, both parent links are consumed regardless of success:

$$m_{t+1}^{12} = m_{t+1}^{23} = -1. \quad (8)$$

With probability p_{sw} , the swap succeeds and the AoE is reset to the sum of link ages $m_t^{12} + m_t^{23}$; otherwise increases by

one in every time slot, after applying the swap-reset rule, and is capped at Δ_{\max} .

$$\Delta_{t+1}^e = \begin{cases} m_t^{12} + m_t^{23}, & \text{w.p. } p_{\text{sw}} \text{ if } a_t^{\text{sw}} = 1, \\ \min(\Delta_t^e + 1, \Delta_{\max}), & \text{otherwise.} \end{cases} \quad (9)$$

If no swap is attempted, $a_t^{\text{sw}} = 0$, elementary link states are determined by

$$m_{t+1}^{12} = g(m_t^{12}), \quad m_{t+1}^{23} = g(m_t^{23}), \quad (10)$$

where $g(m)$ denotes the elementary-link aging operator for $\ell \in \{12, 23\}$.

$$g(m) \triangleq \begin{cases} m + 1, & \text{if } m \in \{1, \dots, m^*\} \text{ and } m + 1 \leq m^*, \\ -1, & \text{if } m \in \{1, \dots, m^*\} \text{ and } m + 1 > m^*, \\ -1, & \text{if } m = -1. \end{cases} \quad (11)$$

Thus, an active elementary link ages by one each time slot and is discarded if its age exceeds m^* .

Regeneration follows a drop-then-attempt rule. If $a_t^{12} = 1$, the (1, 2) link is dropped and replaced by

$$m_{t+1}^{12} = \begin{cases} 1, & \text{w.p. } p_L, \\ -1, & \text{w.p. } 1 - p_L, \end{cases} \quad (12)$$

independently of m_t^{12} . If $a_t^{12} = 0$, then $m_{t+1}^{12} = g(m_t^{12})$. Similarly for m_{t+1}^{23} with a_t^{23} . When both links are requested simultaneously, the success events are conditionally independent.

5) *Reward*: The immediate reward associated with the transition from s_t to s_{t+1} under action a_t is defined as

$$r(s_t, a_t, s_{t+1}) = -\Delta_{t+1}^e. \quad (13)$$

Thus, maximizing reward is equivalent to minimizing the long-term average AoE.

Then, the objective is to determine a stationary policy $\pi : \mathcal{S} \rightarrow \mathcal{A}$ that maximizes the infinite horizon expected average reward

$$\eta^\pi \triangleq \liminf_{T \rightarrow \infty} \frac{1}{T} \mathbb{E}_\pi \left[\sum_{t=0}^{T-1} r(s_t, a_t, s_{t+1}) \right], \quad (14)$$

which equivalently minimizes the expected average AoE.

Next, Theorem 1 establishes that the optimal stationary policy π^* solving the average-reward MDP in (14) can be obtained via Relative Value Iteration (RVI) [12], as summarized in Algorithm 1.

Theorem 1 (Optimal stationary policy and RVI optimality). *For the satellite repeater-chain average AoE minimization problem defined in (14), there exists an average-cost optimal stationary deterministic policy π^* . Moreover, the Relative Value Iteration (RVI) algorithm converges (up to an additive constant), and the resulting stationary policy is optimal.*

Proof. The state of the system $s_t = (v_t^{12}, v_t^{23}, m_t^{12}, m_t^{23}, \Delta_t^e)$ takes values in finite sets; hence the induced average-cost MDP is finite-state and finite-action. Consider the state $(0, 0, -1, -1, \Delta_{\max})$. Because the link visibilities are ergodic

Algorithm 1 Relative Value Iteration (RVI) for AoE Minimization in a Quantum Repeater

Require: State space \mathcal{S} with states $s = (v^{12}, v^{23}, m^{12}, m^{23}, \Delta^e)$; admissible action sets $\mathcal{A}(s)$; transition kernel $P(\cdot | s, a)$ induced by link aging, regeneration, swapping, and visibility dynamics; AoE-based reward function $r(s, a, s') = -\Delta^e$; reference state s_{ref} ; tolerance ε .

Ensure: Optimal stationary policy π^*

- 1: Initialize relative value function $h^{(0)}(s) \leftarrow 0$ for all $s \in \mathcal{S}$
- 2: Initialize policy $\pi^{(0)}(s)$ arbitrarily
- 3: Set iteration index $k \leftarrow 0$

4: **repeat**

5: $k \leftarrow k + 1$

6: **for all** $s \in \mathcal{S}$ **do**

7: **for all** $a \in \mathcal{A}(s)$ **do**

8: Compute

$$Q^{(k)}(s, a) = \sum_{s' \in \mathcal{S}} P(s' | s, a) [-\Delta^{e'}(s') + h^{(k-1)}(s')],$$

where $-\Delta^{e'}(s')$ denotes the AoE component of the next state s' .

9: **end for**

10: Update relative value:

$$h^{(k)}(s) \leftarrow \max_{a \in \mathcal{A}(s)} Q^{(k)}(s, a).$$

11: Update policy:

$$\pi^{(k)}(s) \leftarrow \arg \max_{a \in \mathcal{A}(s)} Q^{(k)}(s, a).$$

12: **end for**

13: **Normalization:**

$$h^{(k)}(s) \leftarrow h^{(k)}(s) - h^{(k)}(s_{\text{ref}}), \quad \forall s \in \mathcal{S}.$$

14: **until** $\max_{s \in \mathcal{S}} |h^{(k)}(s) - h^{(k-1)}(s)| < \varepsilon$

15: **return** $\pi^* \leftarrow \pi^{(k)}$

two-state Markov chains, both links remain invisible for $m^* + (\Delta_{\max} - 1)$ consecutive slots with positive probability. During this period, no new links can be generated, existing links are discarded within m^* slots, and Δ_t^e reaches Δ_{\max} . Thus, $(0, 0, -1, -1, \Delta_{\max})$ is reachable from every state with positive probability under any stationary policy, implying that the MDP is unichain.

For finite-state unichain average-cost MDPs, standard results ([12], Ch. 8) guarantee the existence of an optimal stationary policy and convergence of RVI, completing the proof. \square

IV. SIMULATION RESULTS

This section evaluates the performance of the proposed RVI policy and compares it against two baseline strategies, namely the *Greedy Gen+Swap ASAP* policy and the *Wait-Until-Ready (WUR)* policy, which are commonly used in the quantum

repeater literature due to their simplicity and intuitiveness. We focus on the average AoE as the primary performance metric and examine its behavior under varying elementary link generation probabilities p_L and swap success probabilities p_{sw} under different visibility scenarios.

A. Benchmark Heuristic Policies

The *Greedy Generation + Swap-ASAP* policy attempts to maximize immediate progress toward end-to-end entanglement. At each time slot, the controller behaves as follows:

- If both elementary links (1, 2) and (2, 3) are present, an entanglement swap is attempted immediately, that is, $a^{sw} = 1$.
- Otherwise, the controller requests entanglement generation on all elementary links whenever the satellite is visible, regardless of whether an existing link is already present or not.

The *Wait-Until-Ready* policy adopts a more conservative strategy that avoids unnecessary regeneration when a partial entanglement link already exists. Its behavior is defined as follows:

- If both elementary links (1, 2) and (2, 3) are present, an entanglement swap is attempted immediately, that is, $a^{sw} = 1$.
- If only one elementary link exists, wait for the other elementary link.
- If neither elementary link exists, request entanglement generation on all visible links.
- If the elementary link age is higher than a typical small cut-off time, $\tau = 4$, discard the existing link.

B. Numerical Results

Figure 1 presents the average AoE versus p_L for mostly visible links with $P_{12} = P_{23} = [0.3 \ 0.7; 0.3 \ 0.7]$. For all policies, the AoE decreases as p_L increases due to reduced waiting times for entanglement generation. The RVI policy consistently achieves the lowest AoE across all operating regimes, with the largest performance gains observed at low p_L , where unreliable link generation amplifies the effects of entanglement aging. The Greedy Gen+Swap ASAP policy performs comparably to RVI at high p_L but incurs higher AoE at low and moderate p_L due to myopic swapping and regeneration decisions. In contrast, the Wait-Until-Ready (WUR) policy exhibits the highest AoE, as deferring swapping until both links are available leads to excessive aging in quantum memory, particularly under intermittent link availability.

Figure 2 illustrates the same performance trends under moderately visible links with $P_{12} = P_{23} = [0.6 \ 0.4; 0.4 \ 0.6]$. While the average AoE again decreases with increasing p_L for all policies, the overall AoE levels are higher compared to the mostly visible case in Fig. 1, reflecting the reduced satellite availability. Nevertheless, the RVI policy continues to outperform both baseline strategies across all regimes, highlighting its robustness to degraded visibility conditions.

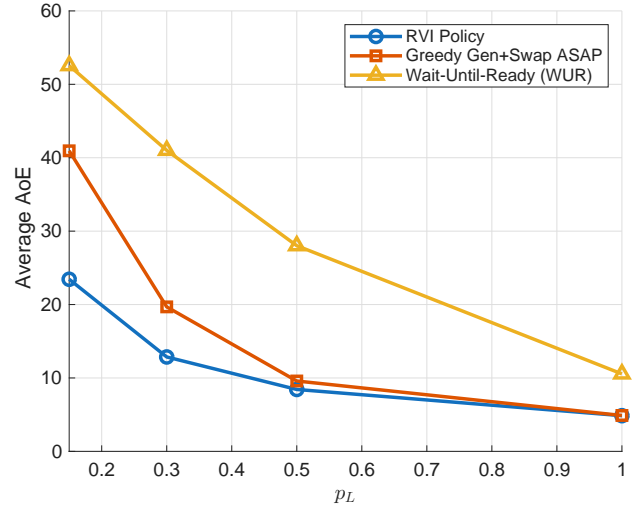


Fig. 1. Average age of entanglement (AoE) versus the elementary link generation probability p_L under mostly visible links with visibility transition matrices $P_{12} = P_{23} = [0.3 \ 0.7; 0.3 \ 0.7]$, when $p_{sw} = 0.8$.

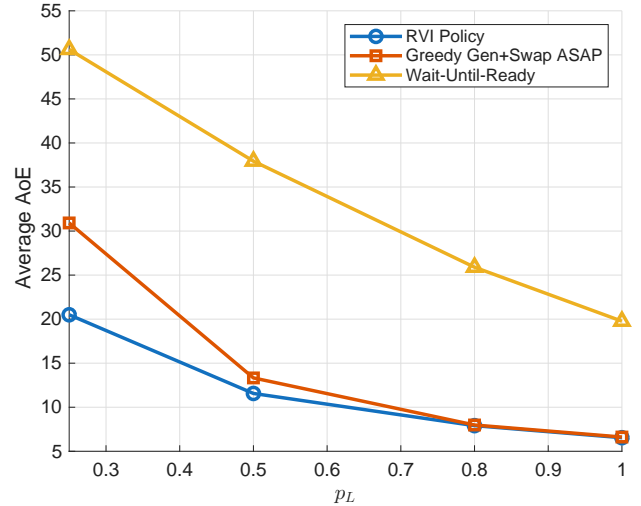


Fig. 2. Average age of entanglement (AoE) versus elementary link generation probability p_L under moderately visible links with visibility transition matrices $P_{12} = P_{23} = [0.6 \ 0.4; 0.4 \ 0.6]$, when $p_{sw} = 0.8$.

Figure 3 shows the average AoE as a function of the swap success probability p_{sw} for a fixed link generation probability $p_L = 0.3$ under asymmetric visibility conditions. The visibility processes are given by $P_{12} = [0.1 \ 0.9; 0.1 \ 0.9]$ and $P_{23} = [0.55 \ 0.45; 0.55 \ 0.45]$, indicating that the first link is frequently visible while the second is more intermittent. As p_{sw} increases, the AoE decreases for all policies due to reduced waiting in quantum memory. The RVI policy consistently achieves the lowest AoE, while the Greedy policy degrades at low and moderate p_{sw} , and the Wait-Until-Ready (WUR) policy incurs the highest AoE due to longer storage under asymmetric link availability. Asymmetric link availability also degrades the optimal performance achieved by RVI algorithm.

The convergence behavior of the proposed RVI algorithm is

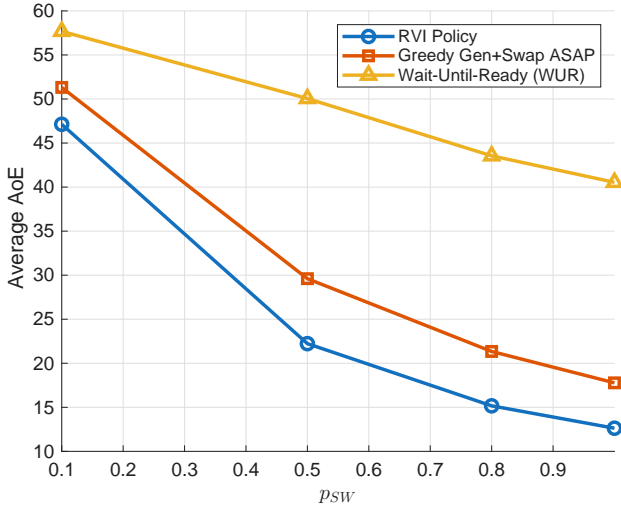


Fig. 3. Average age of entanglement (AoE) versus swapping success probability p_{sw} under asymmetric visibility with visibility transition matrices $P_{12} = [0.1 \ 0.9; 0.1 \ 0.9]$ and $P_{23} = [0.55 \ 0.45; 0.55 \ 0.45]$, when $p_L = 0.3$.

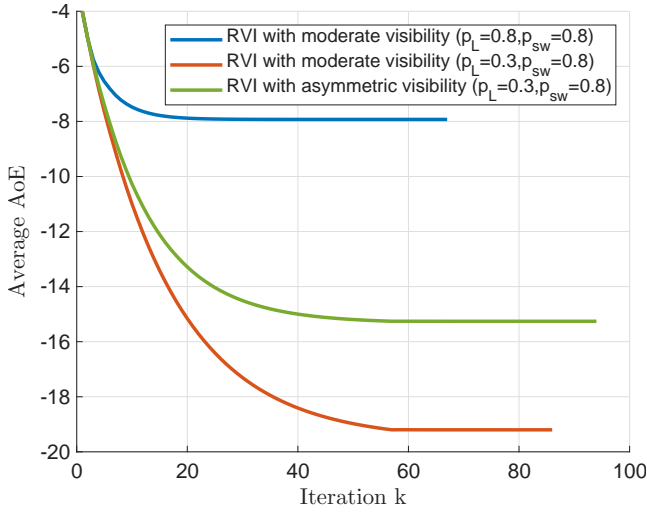


Fig. 4. Convergence of the Relative Value Iteration (RVI) algorithm under different scenarios.

shown in Fig. 4. As p_L and p_{sw} decrease, convergence slows slightly but remains within a reasonable number of iterations.

V. CONCLUSION

This paper has investigated the control of continuous entanglement distribution in satellite-assisted quantum networks under probabilistic operations, intermittent visibility, and quantum memory decoherence. By modeling entanglement freshness using the novel AoE metric and formulating the problem as an average-cost Markov decision process, we have demonstrated that state-aware control policies can significantly outperform greedy and conservative baseline strategies across a wide range of operating conditions. The proposed RVI-based policy consistently achieves lower AoE by accounting for future costs and heterogeneous link dynamics, particularly

in regimes characterized by low link reliability or asymmetric visibility. By keeping entanglement fresh and optimally allocating actions, this work advances the design of efficient and reliable quantum networking systems. This work also provides a baseline for future studies on AoE optimization in longer repeater chains and possibly the development of learning-based control algorithms to enable more scalable solutions in large-scale quantum networks.

REFERENCES

- [1] H.-J. Briegel, W. Dür, J. I. Cirac, and P. Zoller, “Quantum repeaters: The role of imperfect local operations in quantum communication,” *Phys. Rev. Lett.*, vol. 81, pp. 5932–5935, Dec 1998. [Online]. Available: <https://link.aps.org/doi/10.1103/PhysRevLett.81.5932>
- [2] S.-K. Liao, W.-Q. Cai, W.-Y. Liu *et al.*, “Satellite-to-ground quantum key distribution,” *Nature*, vol. 549, pp. 43–47, 2017.
- [3] J. S. Sidhu, S. K. Joshi, M. Gündoğan, T. Brougham, D. Lowndes, L. Mazzarella, M. Krutzik, S. Mohapatra, D. Dequal, G. Vallone, P. Villoresi, A. Ling, T. Jennewein, M. Mohageg, J. G. Rarity, I. Fuentes, S. Pirandola, and D. K. L. Oi, “Advances in space quantum communications,” *IET Quantum Communication*, vol. 2, no. 4, p. 182–217, Jul. 2021. [Online]. Available: <https://doi.org/10.1049/qtc2.12015>
- [4] Z. Yang, K. Cai, Z. Chen, and J. Zhang, “Optimizing satellite-to-ground station pair assignments using hybrid links for long-distance quantum entanglement distribution,” *IEEE Communications Letters*, vol. 30, pp. 322–326, 2026.
- [5] S. Kaul, R. Yates, and M. Gruteser, “Real-time status: How often should one update?” in *2012 Proceedings IEEE INFOCOM*, 2012, pp. 2731–2735.
- [6] R. D. Yates, Y. Sun, D. R. Brown, S. K. Kaul, E. Modiano, and S. Ulukus, “Age of information: An introduction and survey,” *IEEE Journal on Selected Areas in Communications*, vol. 39, no. 5, pp. 1183–1210, 2021.
- [7] A. Kolar, A. Zang, J. Chung, M. Suchara, and R. Kettimuthu, “Adaptive, continuous entanglement generation for quantum networks,” in *IEEE INFOCOM 2022 - IEEE Conference on Computer Communications Workshops (INFOCOM WKSHPS)*, 2022, pp. 1–6.
- [8] Á. G. Iñesta and S. Wehner, “Performance metrics for the continuous distribution of entanglement in multi-user quantum networks,” *Physical Review A*, vol. 108, no. 5, p. 052615, 2023, arXiv preprint [arXiv:2307.01406v2](https://arxiv.org/abs/2307.01406v2).
- [9] S. Haldar, P. J. Barge, S. Khatri, and H. Lee, “Fast and reliable entanglement distribution with quantum repeaters: Principles for improving protocols using reinforcement learning,” *Physical Review Applied*, vol. 21, no. 2, p. 024041, 2024.
- [10] G. X. Yau, A. Burushkina, F. F. d. Silva, S. Majit, P. S. Thomas, and G. Vardoyan, “Reinforcement learning for quantum network control with application-driven objectives,” *arXiv preprint arXiv:2509.10634v1*, 2025.
- [11] M. Chehimi, K. Goodenough, W. Saad, D. Towsley, and T. X. Zhou, “Entanglement distribution delay optimization in quantum networks with distillation,” *IEEE Journal on Selected Areas in Communications*, vol. 43, no. 5, pp. 1871–1886, 2025.
- [12] M. L. Puterman, *Markov Decision Processes: Discrete Stochastic Dynamic Programming*. New York: John Wiley & Sons, 1994.
- [13] S. Haldar, P. J. Barge, X. Cheng, K.-C. Chang, B. T. Kirby, S. Khatri, C. W. Wong, and H. Lee, “Reducing classical communication costs in multiplexed quantum repeaters using hardware-aware quasi-local policies,” *Communications Physics*, vol. 8, no. 1, 2025, arXiv preprint [arXiv:2401.13168v3](https://arxiv.org/abs/2401.13168v3).
- [14] E. T. Ceran, D. Gündüz, and A. György, “Average age of information with hybrid arq under a resource constraint,” *IEEE Transactions on Wireless Communications*, vol. 18, no. 3, pp. 1900–1913, 2019.
- [15] Y. Sun, I. Kadota, R. Talak, and E. Modiano, *Age of Information: A New Metric for Information Freshness*, 1st ed. Springer, 2020.